Involvement of Contractile Proteins in the Changes in Consistency of Oocyte Nucleoplasm of the Newt *Pleurodeles waltlii*

PIERRE GOUNON and ERIC KARSENTI

Centre de Cytologie Experimentale du Centre National de la Recherche Scientifique, 94200 Ivry-sur-Seine, France; Laboratoire de Biologie du Développement, Université Pierre et Marie Curie, Paris, France; and Laboratoire d'Immunocytochimie, Institut Pasteur, Paris, France

ABSTRACT In the present work, we show that actin is present in considerable quantities in the oocyte nucleus of the newt *Pleurodeles waltlii*. The nuclear sap, extracted in saline buffer containing Ca^{++}, is fluid. DNAase I inhibition assays have shown that 90% of actin is under a globular state in such conditions. Chelation of Ca^{++} by EGTA leads to the formation of a nuclear gel composed of individual microfilaments. This nuclear gel contains ~50% of total nuclear actin in a filamentous form. Phalloidin, a drug known to stabilize F-actin, induces the formation of a network of actin cables in the nuclei. This network contains nearly 100% of total nuclear actin in the filamentous form. The observation of the cables in the electron microscope shows that they are made of tightly associated microfilaments to which RNP-like particles are bound. The actin antibodies stain the cables and the particles by the indirect immunoperoxidase technique; myosin antibodies mainly stain the particles. The formation of the phalloïdin-induced network seems to require the presence of Ca^{++}, Mg^{++}, and ATP. We propose a scheme for the regulation of the supramolecular forms of actin in oocyte nuclei in which a delicate equilibrium seems to exist between globular actin, microfilaments, and actin cables. This equilibrium would be controlled by the concentration of Ca^{++}, ATP, and various actin-associated proteins.

The presence of actin, myosin, and other actin-associated proteins as major components of nonhistone proteins in interphase nuclei has been reported by several authors (7, 9, 11, 26, 34, 36). Moreover, it has been found that the induction of a nonproliferative state in various cell types is followed by an increase in the concentration of an actinlike protein in the nucleus, which is concomitant with chromatin condensation (25). The immunocytochemical approach that we have applied to lampbrush chromosomes, which are present in the nucleus of oocytes of the newt *Pleurodeles*, has shown that actin, at least, could be found associated with a highly condensed state of chromatin; the chromomeres of lampbrush chromosomes (21). Moreover, these chromosomes were found to contract to half their normal size in the presence of ATP, suggesting that normal chromosome condensation could involve an actomyosin contractile matrix (20). This proposition has been recently supported by the finding that *in situ* condensation of chromosomes in *Xenopus laevis* oocytes could be inhibited by anti actin antibodies injected into the nucleus (37). These nuclei have been shown to contain actin in a soluble diffusible form and in the form of an insoluble nuclear gel in which nucleoli and chromosomes are embedded (5, 6). In fact, Callan (3) states "there is great variation in the physical consistency of the nuclear sap of oocytes of different organisms, and considerable variation, known to be related to physiological state, in anyone species". As a consequence, "some organisms lend themselves readily to lampbrush chromosome study, others are refractory" (3). It was found, however, that the very stiff nuclear sap of axolotl could be dispersed in a saline containing 10^{-5}–5×10^{-5} M $CaCl_2$, allowing the preparation of well spread lampbrush chromosomes (4). Thereafter, $CaCl_2$ was routinely added to the media used to prepare lampbrush chromosomes from other species to obtain well spread preparations. In *Pleurodeles waltlii*, a strain of newt which has been maintained in the laboratory for 30 yr, the nuclear sap is rather fluid, at least during the reproductive phase of this species (between

THE JOURNAL OF CELL BIOLOGY · VOLUME 88 FEBRUARY 1981 410-421

September and April in the laboratory), allowing the preparation of well spread lampbrush chromosomes.

The present work deals with the study of the structural state of the nuclear sap of the newt *Pleurodeles waltlii*, isolated under various conditions. Our results indicate that contractile proteins, mainly actin and possibly myosin, are involved in the structure of the nuclear sap. Moreover, the dispersal effect of Ca^{++} on the nuclear sap is tentatively attributed to an effect of this cation on the level of actin polymerization and microfilament cross-linking.

MATERIALS AND METHODS

Isolation of Nuclei

Nuclei were isolated from the newt *Pleurodeles waltlii* (Amphibia, Urodela) oocytes as previously described (20, 21). After ovarian biopsy, an oocyte was ruptured with fine forceps and a tungsten needle in a sterile saline medium (0.08 M KCl, 0.02 M NaCl in distilled water). The nucleus was freed of its yolky cytoplasm with a calibrated Pasteur pipette and transferred to an observation chamber containing 25 μl of Tris-buffered saline (TBS) consisting of 0.08 M KCl, 0.02 M NaCl, 10^{-3} M $MgCl_2$, and 5×10^{-5} M $CaCl_2$ in 0.02 M Tris-HCl, pH 7.2. The nuclei were treated with ATP, ATP analogs, phalloidin, or cytochalasin B, as described previously (20), either before or after removal of the nuclear membrane. The nuclear material was then centrifuged to the bottom of the chambers for 5 min at 50 *g* and 25 min at 2,000 *g* in a Sorvall RC2B (DuPont Instruments-Sorvall, Dupont Co., Newtown, Conn.), using swinging buckets and tubes with an adaptor for the chambers.

Electron Microscopy

The observation chambers, containing centrifuged nuclear material, were immersed in glutaraldehyde (1% in TBS) or OsO_4 (0.5% in TBS) for 15 min, washed rapidly with TBS, and dehydrated with serial concentrations of ethanol. The bottom coverslips of the chambers were then removed, and capsules filled with Araldite were gently poured onto the coverslips. After the Araldite had polymerized, the coverslips were removed by freezing in liquid nitrogen. Proteins were localized on the surface of the blocks by rapid staining with a mixture of 1/1-methyl blue and azur B (vol/vol) at 60°C. Ultrathin sections were cut with a diamond knife on a Reichert ultramicrotome (Reichert Jung, Vienna, Austria), mounted on uncoated copper grids, and observed with a Philips electron microscope 201, (40, 60, or 80 keV). Sections were stained with lead citrate and uranyl acetate except for the material treated by the immunoperoxidase technique. Unfixed samples of nuclear proteins were also adsorbed onto hydrophilic Formvar carbon-coated grids and stained with 1% uranyl acetate.

Antigens

PURIFICATION OF ACTIN: Actin was purified according to the method of Spudich and Watt (38) from frog leg muscles (*Rana ridibunda*). Four cycles of polymerization-depolymerization were necessary to obtain pure actin. This purity was judged by SDS polyacrylamide slab gel electrophoresis (8.75 and 12.5% acrylamide), according to Laemmli (24) (Fig. 1).

PURIFICATION OF MYOSIN: Myosin was purified by a two-step procedure, adapted from Mommaerts and Parrish (32) and from Pollard et al. (35), from frog *Rana* leg muscles. 40 g of muscle were minced in a meat grinder and extracted (12 mn) with buffer I (0.3 M KCl, 0.075 M KH_2PO_4, 0.075 M K_2HPO_4, 0.02 M EDTA, 0.005 M Mg acetate, 0.1 mM phenylmethylsulfonyl flouride [PMSF]). The extract was then diluted threefold with distilled water and clarified by filtration through gauze and low speed centrifugation. The resulting supernate was diluted 10-fold with distilled water and then incubated for 18 h at 0°C to allow for precipitation of the crude myosin. After centrifugation, the supernate was discarded and the pellet dissolved in buffer II (0.5 M KCl, 0.05 M K_2HPO_4, 0.05 M KH_2PO_4, 5 mM Mg SO_4, 0.1 mM PMSF, 0.5 mg/ml ATP). This solution was then centrifuged (110,000 *g* for 30 min) and the myosin preparation was dialyzed against 10 mM Tris-HCl, pH 7.5, 0.1 M KCl, 1 mM $MgCl_2$ to form thick synthetic filaments (39).

After centrifugation, the pellet of thick filaments was dissolved in buffer III (10 mM Tris-HCl, pH 7.5, 1 mM EDTA, 0.1 mM dithiothreitol (DTT), 0.6 M KI, 5 mM ATP, 5 mM $MgCl_2$, 1 mM $CaCl_2$). The solution was clarified by centrifuging at 100,000 *g* and immediately applied to the gel filtration column described below. A 2.6 × 120-cm column was packed with acrylamide-agarose beads (AcA22 Biogel-Bio-Rad Laboratories, Richmond, Calif.) using gravity flow with a 40-cm pressure head and equilibrated with column buffer (10 mM Tris, pH 7.5, 1 mM EDTA, 0.1 mM DTT, 0.6 M KCl, 0.2 mM ATP). 20 ml of buffer III were applied to the column followed by 30 mg of protein in 10 ml of buffer III and then by 10 ml of buffer III alone. Elution was carried out with column buffer. Two major peaks were eluted from the column. The first one contained myosin and the second one predominantly actin. The myosin pool was concentrated by forming thick filaments which were pelleted by centrifugation (17,000 *g* for 30 min). The pellet was dissolved by adding 3 M KCl to obtain a final concentration of 0.6 M KCl. The purity of myosin was judged by SDS slab gel electrophoresis (8.5% acrylamide) according to Laemmli (see Fig. 1).

Preparation of Antisera

ACTIN ANTISERUM: In this work, we have used two different actin antibodies. One antibody was directed against actin from calf striated muscle purified by SDS polyacrylamide gel electrophoresis. The immunization of the rabbit and the preparation and characterization of this antibody have been described elsewhere (23). The other antibody was prepared against frog (*Rana ridibunda*) actin. A rabbit was immunized against this actin preparation without SDS, according to the method described by Jockush et al. (19). 0.3 mg of native actin, emulsified in complete Freund's adjuvant, was injected into the foot pads on day 1 and into the back on day 10. The following injections were applied intravenously with alum ($KAl\ [SO_4]_2$)-adsorbed actin (19): days 25, 27, and 31, 0.1 mg of protein; days 40, 42, and 44, 0.2 mg of protein. A double immunodiffusion test was carried out with serum taken on day 54, and a single precipitin line was observed when actin was used between 2.5 and 0.6 mg/ml. At lower actin concentrations, no precipitin line was detected. The rabbit was bled on day 57 and gave 40 ml of serum, which was frozen at −20°C.

MYOSIN ANTISERA: Two rabbits were immunized against Frog (*Rana ridibunda*) myosin, according to the following procedure: 1 mg of myosin emulsified in complete Freund's adjuvant was injected into the foot pads of the rabbits on day 1. The following injections were applied in the back, with 0.5 mg of myosin emulsified in complete Freund's adjuvant, on days 30, 53, 81, and 104. The sera were routinely tested by double immunodiffusion 1 wk after each injection. The first precipitation reaction was observed after the second injection of myosin. The rabbits were bled 1 wk after the last injection. The sera obtained from each bleeding were individually frozen at −20°C.

Antibody Purification

Actin-Sepharose and myosin-Sepharose columns were prepared according to Cuatrecasas et al. (8). Actin and myosin (1.5 mg/ml) were dialyzed overnight against 0.5 M KCl, 0.1 M $NaHCO_3$, pH 8.5, at 4°C and mixed with CNBr-activated Sepharose (Sepharose 4B, Pharmacia Fine Chemicals, Sweden) for 2 h under rotating agitation at room temperature. The gels were centrifuged, and the absorption (280 nm) of the supernate was measured to estimate the amount of protein bound to the gel. The immunoadsorbants were washed three times in the coupling buffer, until the optical density 280 of the supernate was <0.005, and then resuspended in 1 M ethanolamine, pH 8.0, for 1 h at room temperature. The immunoadsorbants were then repeatedly washed in 0.1 M borate, pH 8.5, alternating with 0.1 M acetate, pH 4.0, containing 0.5 M KCl. Finally, the gels were taken up in a Phosphate-buffered saline (PBS) buffer (0.01 M potassium-phosphate pH 7.4, 0.15 M NaCl). The actin-Sepharose immunoadsorbant contained 21 mg of protein. The myosin-Sepharose immunoadsorbant contained 11 mg of protein. The two columns were extensively washed with PBS until the pH of the elution fluid was 7.1–7.2.

In addition to purifying the antigen used, we decided to run the actin antiserum on a myosin column before purification of antibodies on the actin column to eliminate any possible contamination of the purified anti actin by myosin antibodies. The same was done for the myosin antiserum, in the reversed order.

Actin antibodies were, therefore, purified in the following way: 20 ml of actin antiserum were run (30 ml/h) at room temperature on the column of Sepharose 4B-myosin which was directly connected to the column of Sepharose 4B-actin. The two columns were then washed separately with PBS at room temperature. When the absorbance of the effluent at 280 nm was close to zero, the columns

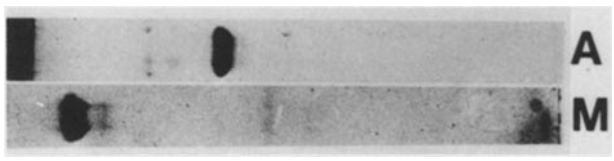

FIGURE 1 Electrophoretic analysis of myosin and actin preparations. Track *M* (myosin) was cut from a 8.75% SDS polyacrylamide slab gel. Track *A* (actin) was cut from a 12.5% SDS polyacrylamide slab gel. Proteins were stained with Coomassie Blue.

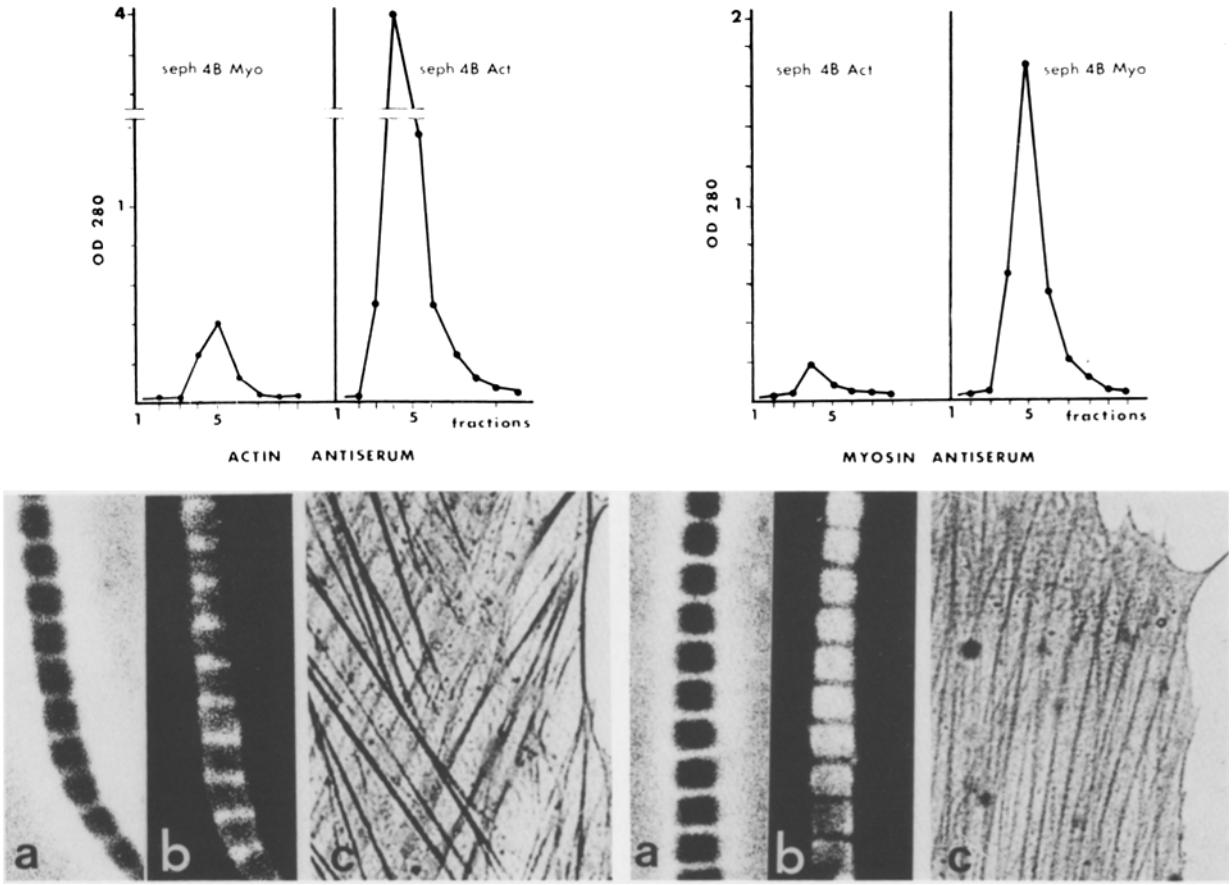

FIGURE 2 Affinity column purification and specificity test of actin and myosin antibodies. Left; the actin antiserum was run successively through the myosin and the actin affinity columns. The antibodies eluted from the actin affinity column stained the I bands of *Rana* skeletal muscle myofibrils in indirect immunofluorescence. *a*, Phase contrast microscopy of a myofibril; *b*, fluorescence microscopy of the same myofibril (× 2,950); *c*, the same antibodies stained the stress fibers of mouse fibroblasts by the indirect immunoperoxidase technique. × 1,700. Right; the myosin antiserum was run successively through the actin and the myosin affinity columns. The antibodies eluted from the myosin affinity column stained the A bands of *Rana* skeletal muscle myofibrils in indirect immunofluorescence. *a*, Phase contrast microscopy of a myofibril; *b*, fluorescence microscopy of the same myofibril (× 2,950); *c*, the same antibodies stained the stress fibers of mouse fibroblasts by the indirect immunoperoxidase technique. In this case a faint dotted staining could be seen. × 1,700.

were transferred to 4°C. Antibodies were eluted with a 4 M $MgCl_2$ solution. Antibodies were immediately dialyzed at 4°C against 5 liters of PBS for 3 h and overnight against 5 liters of PBS containing 30% glycerol. At the end of dialysis, the concentration of proteins eluted from the column of actin (antiactin) was 1.4 mg/ml; the total amount of protein was 14 mg. The concentration of proteins eluted from the column of myosin was 0.18 mg/ml; the total amount of protein was 1.4 mg.

Myosin antibodies were purified by the same procedure. 20 ml of myosin antiserum were run on the column of actin directly connected to the column of myosin. After dialysis, the concentration of proteins eluted from the column of myosin (antimyosin) was 0.5 mg/ml. Total amount of protein was 10 mg. The concentration of proteins eluted from the column of actin was 0.07 mg/ml. Total amount of protein was 1 mg. the elution profiles shown in Fig. 2 clearly demonstrate that the antisera contained very few, if any, heterospecific antibodies.

Rabbit anti-rat IgG purified on a column of rat IgG coupled to glutaraldehyde-activated acrylamide-agarose beads (ACA 3-4) according to Ternynck and Avrameas (40) was a gift of J.-C. Antoine (Institut Pasteur, Paris). These antibodies were used in control experiments.

Antibody Characterization

Purified actin and myosin antibodies were tested by indirect immunofluorescence on frog leg muscle myofibrils as described by Herman and Pollard (17). Myofibrils prepared and kept at −20°C in rigor buffer (0.1 M KCl, 2 mM $MgCl_2$, 0.1 mM EGTA, 10 mM imidazol, 1 mM DTT, pH 7.0) containing 50% glycerol were washed by centrifugation in rigor buffer containing 10% glycerol, resuspended in purified antibodies (30 μg/ml in rigor buffer containing 10% glycerol), and incubated for 1 h at room temperature. The myofibrils were then centrifuged, washed once in rigor-glycerol buffer, and incubated for a further hour at room temperature in fluorescein-tagged sheep anti-rabbit IgG (30 μg/ml in rigor-glycerol buffer). After two washes, the myofibrils were observed on a Zeiss microscope equipped with epifluorescence illumination. As shown in Fig. 2, antiactin stained the I bands whereas antimyosin stained the A bands, demonstrating further the specificity of the antibodies. The proteins, adsorbed in low amount on the column of myosin from the actin antiserum, did not stain the myofibrils even at concentrations >200 μg/ml. The proteins adsorbed on the column of actin from the myosin antisera at concentration >200 μg/ml weakly stained the I bands of myofibrils. This may indicate that a small amount of actin antibodies were present in this antiserum. These may be natural antibodies (10, 13, 22, 33). Our purified antibodies which were raised against muscle actin and myosin were also tested on mouse fibroblastic cells to determine whether they could recognize antigenic determinants present on the corresponding nonmuscle proteins. We used a mouse fibroblastic cell line (3/A/1-D3) isolated by Dr. J.-F. Nicolas, Institut Pasteur, Paris. The test was carried out using the immunoperoxidase technique previously described (23). Fig. 2 shows that the stress fibers are stained in a typical way by actin and myosin antibodies used at 60 μg/ml. Moreover, both antibodies were found to stain smooth muscles on frozen sections of quail oviduct (data not shown).

Immunocytochemical Staining of Phalloidin-treated Nuclear Sap

A nucleus was ruptured in an observation chamber containing phalloidin (10^{-4} M). After incubating for 10 min at room temperature, the chamber was centrifuged (50 *g* for 5 min and 2,200 *g* for 30 min). The preparation was then gently washed in TBS and incubated with 15 μl of purified antibodies (diluted in

TBS; 30 μg/ml final concentration) for 1 h at room temperature in a humidified atmosphere. The preparation was extensively washed in a slotted box containing TBS and incubated for a further hour at room temperature in 15 μl of purified, peroxidase-labeled sheep anti-rabbit IgG antibodies (15 μg/ml) (Institut Pasteur, Paris). After washing extensively in TBS, the peroxidase activity was revealed by incubation of the chamber for 10 min in a diaminobenzidine (DAB) solution (5 mg of DAB, 10 ml of Tris-HCl 0.1 M pH 7.6, 0.03% H_2O_2) (14). The preparation was finally washed with TBS, mounted in glycerin jelly (Difco Laboratories, Detroit, Mich.) for light microscopy, or processed for electron microscopy as described above.

S_1 Myosin Subfragment Decoration of Phalloidin-and EGTA-treated Nuclear Sap

Purified rabbit S_1 myosin subfragment was a gift of Dr. R. Whalen, Institut Pasteur, Paris, France.

Nuclei were isolated in TBS containing phalloidin (10^{-4} M) or EGTA (10 mM) in the presence of rabbit S_1 myosin subfragment (1 mg/ml). The nuclear envelope was removed, and after 15 min of incubation at room temperature the nuclear sap was centrifuged to the bottom of the chamber. After washing in TBS, the material was fixed in TBS containing glutaraldehyde (1%) and tannic acid (0.2%) for 10 min. Araldite embedding was then carried out as described above.

DNAase I Inhibition Assays

The tests were carried out according to Blikstad et al. (1) and Clark and Rosenbaum (6). All the buffers are described in those papers. Briefly, 20 μl (2 μg) of a diluted stock solution of DNAase I (Sigma Chemical Co., DN-EP) were mixed with 20 μl of the sample by strong agitation and immediately diluted in 3 ml of substrate (calf thymus DNA, Sigma Type I, 40 μg/ml).

The hyperchromicity at 250 nm was recorded in a Jobin-Yvon spectrophotometer (Jobin-Yvon, Arcucil, France). Measurements were made in the 30–70% inhibition of the standard amount of DNAase I. Each assay was carried out using at least five hand-isolated nuclei. The amount of G-actin present in nuclei isolated in 20 μl of K/Na solution, TBS/EGTA (10 mM), or TBS containing phalloidin (10^{-4} M) was measured by calculating the percent of inhibition of DNAase I activity in each case relative to control assays containing 20 μl of the medium in which the nuclei were prepared. Total nuclear actin (G + F-actin) was measured by disrupting nuclei in 20 μl of the actin depolymerizing medium containing 1.5 M guanidine hydrochloride (Gu-HCl) described by Blikstad et al. (1). The absolute amount of actin present in oocyte nuclei was calculated from a standard inhibition curve of DNAase I activity measured in the presence of known quantities of purified *Rana* skeletal muscle actin. The inhibition of enzyme activity measured for total actin from a given number of nuclei was compared with the standard curve, and the absolute amount of actin/nucleus was calculated.

Chemicals

ATP (disodium salt) and RNase A and T1 were purchased from Sigma Chemical Co. ATPγS, ATP (β-γNH) disodium salt and phalloidin were purchased from Boehringer Mannheim Biochemicals, Indianapolis, Ind. Cytochalasin B (Boehringer Mannheim Biochemicals) was dissolved in dimethyl sulfoxide (DMSO) before use. 0.1 M stock solutions of EDTA and EGTA (Sigma Chemical Co.) were made in distilled water and dissolved by neutralisation to pH 7.3.

RESULTS

Structure of the Nuclear Sap in Nuclei Isolated in TBS

In *Pleurodeles* oocytes, the nuclear sap is usually fluid, and freshly isolated nuclei are translucent in K/Na solution and in TBS (Fig. 3*a*). After 30 min of incubation in TBS at room temperature, the nuclei become more opaque but the nuclear sap spreads well in the chamber upon removal of the nuclear envelope, indicating that it has remained fluid. In phase contrast microscopy, only lampbrush chromosomes, nucleoli, and a slightly granular material can be observed.

The structure of the nuclear sap centrifuged on a coverslip in TBS embedded in Araldite and observed in the electron microscope after fixation in glutaraldehyde containing tannic acid is shown in Fig. 4*a*. Very few microfilaments are visible, except near nucleoli around which microfilaments associated with electron-dense particles can be distinguished (Fig 4*a*, inset). The same pictures can be obtained in nuclei centrifuged in K/Na immediately upon isolation.

A representative picture of a freshly isolated (<1 min) nuclear sap, adsorbed to an electron microscope grid and stained with uranyl acetate, is shown in Fig. 4*b*. No obvious filaments or cables are visible. The predominant material consists of granular structures with a size range of 20–50 nm. Larger particles, up to 300 nm, correspond to aggregate 20–50-nm granules. Nucleoli and chromosomes were sometimes present on the grids.

Structure of the Nuclear Sap in Nuclei Treated by Phalloidin in TBS

In the presence of phalloidin, a drug which stabilizes F-actin in vivo and in vitro (27, 42, 43), the oocyte nucleus becomes slightly opalescent (Fig. 3*b*). This opalescence appears slowly and the final state is reached after 10–15 min of incubation. When observed by phase contrast microscopy, after removal of the nuclear envelope, the nuclear sap appears to consist of a network of intricated fibrils (Fig. 5*a*). Cytochalasin B (10 μg/ml) antagonizes the phalloidin effect but does not dissociate previously formed networks. The structure of the network of fibrils observed by electron microscopy after Araldite embedding and thin sectioning is shown in Fig. 5*b*. Cables, 30 nm in diameter, associated in bundles, up to 300 nm in size, are visible. The cables are covered with a electron-dense granular material. S_1 myosin subfragment decorates the cables as shown in Fig. 5*c*.

To determine the molecular structure of these cables, samples were spread on a water drop, adsorbed on a grid, and stained with uranyl acetate (Fig. 5*d* and *e*). Filaments 6–7 nm in diameter, in which a subunit organization can be distinguished, are found most often associated into cables (20–30 nm) on which particles (100–300 nm) containing ill-defined subunits (20 nm) are bound. Numerous ring structures ~10 nm in diameter are visible between the cables (Fig. 5*e*, small arrows and inset).

Nuclei treated with phalloidin become rigid spheres. Removal of the nuclear membrane and centrifugation for 30 min onto a glass coverslip does not disperse the nuclear material that remains embedded in the polymerized matrix (Fig. 6).

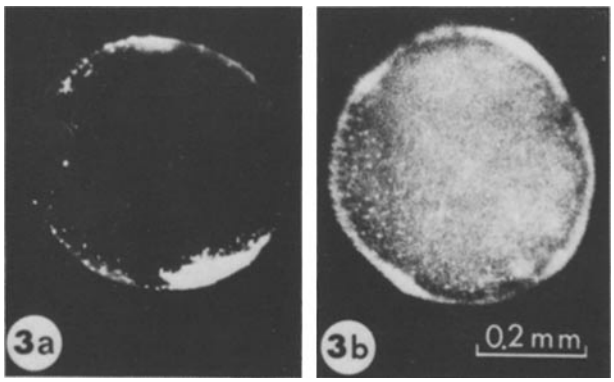

FIGURE 3 Oocyte nuclei observed under the binocular lens. × 75. (*a*) A nucleus freshly isolated in TBS is shown. Note the translucent appearance of the nucleoplasm. The white material visible on the surface of the nucleus corresponds to yolk platelets. (*b*) A nucleus treated by phalloidin (10^{-4} M) for 15 min. The nucleoplasm becomes opalescent.

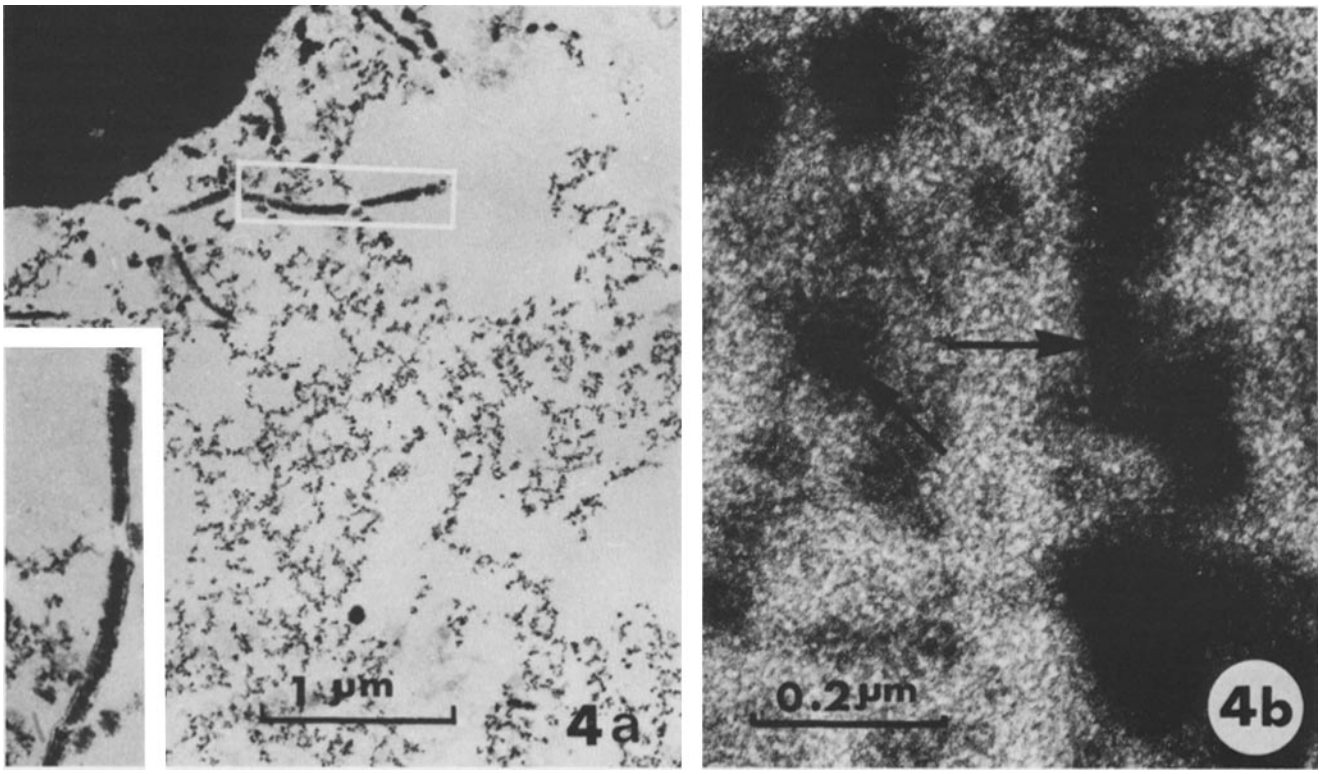

FIGURE 4 The nuclear sap of freshly isolated nuclei. (*a*) The nuclear sap was embedded in Araldite after fixation with 1% glutaraldehyde, 0.2% tannic acid, and observed by transmission electron microscopy. × 25,000; *inset*, × 62,000. Note the slightly granular aspect of the nuclear sap and the particles aggregated between microfilaments, near nucleoli (see *inset*). (*b*) A sample of nuclear sap was adsorbed on a formvar carbon-coated grid, stained with uranyl acetate (1%-2 min), and observed by electron microscopy. × 130,000. Note the aggregated 20–50-nm particles (arrows).

Treatment of such preparations with actin antibodies by the indirect immunoperoxidase technique (Fig. 6*a*) shows that the whole network, the chromosomes (arrowheads) and nucleoli (arrows), are stained. By contrast, antimyosin (Fig. 6*b*) does not decorate the network and stains the chromosomes only faintly. The apparent high contrast of the nucleoli is caused by their intrinsic refringence, as is demonstrated by observation at higher magnifications (data not shown). Observation of antiactin-stained networks at higher magnification (Fig. 7*a*) shows a rather smooth and uniform staining localized directly on the fibers. At the same concentration, antimyosin stains granules evenly distributed on the bottom of the observation chamber, and a slight dotted staining seems to be localized on the fibers (Fig. 7*b*). Such a staining is absent from control preparations in which antiactin or antimyosin was replaced by a rabbit anti-rat IgG (Fig. 7*c*).

Electron microscopic images of nuclear networks treated by anti-IgG (controls), antimyosin, and antiactin antibodies are shown in Fig. 8. The preparations were observed at 40 or 60 keV to enhance the contrast of the diaminobenzidine precipitate over the intrinsic contrast of proteins. The usual contrast of proteins observed on sections of networks treated with IgG antibodies instead of antimyosin or antiactin is shown in Fig. 8*a*. When myosin antibodies are applied to the preparations, dark dots of staining are found associated with the particles bound to the cables (Fig. 8*b*). A faint staining is also visible in some places on the cables. The actin antibodies stain the filaments, the cables, and the associated particles (Fig. 8*c*).

Structure of the Nuclear Sap in Low Ca^{++} Concentration

The effect of the divalent cation chelators EDTA and EGTA on the structure of the nuclear sap is not the same. In the

FIGURE 5 Phalloidin-induced networks of fibers in the nucleoplasm. Isolated nuclei were treated for 15 min with phalloidin (10^{-4} M). After removal of the nuclear envelope, the networks were centrifuged onto a glass coverslip (see Materials and Methods) and observed by (*a*) phase contrast microscopy, × 1,700, or (*b*) embedded in Araldite and observed by electron microscopy after thin sectioning. × 6,000. S_1 myosin subfragment (1 mg/ml) was added in *c*. × 100,000. The network of large fibers visible in phase contrast microscopy (*a*) is made up of bundles of cables (*b*) covered with a granular electron-dense material. S_1 arrowhead decoration of cables is shown in *c*. A sample of the network adsorbed to a Formwar carbon-coated grid and stained with uranyl acetate (1% for 2-min) is shown in *d* (× 25,000) and *e* (× 180,000, *inset* × 200,000). In *f*, ATPγS (1-mM) was added to a network 3 min after the addition of phalloidin and maintained for 5 min before processing for electron microscopy. × 180,000. The experiment was monitored by phase contrast microscopy. This figure corresponds to the state in which the network could no longer be visualized by phase contrast microscopy. Note the cables made up of numerous, tightly associated (6–7 nm) filaments (*d* and *e*), the large particles made of 20–30-nm subunits, heavily stained by uranyl acetate (Fig. *d* and *e*, arrowheads) and the ring structures 10 nm in diameter (*e*, small arrows and inset). Cables dissociated into 6–7-nm filaments by ATPγS are shown in *f* (arrows).

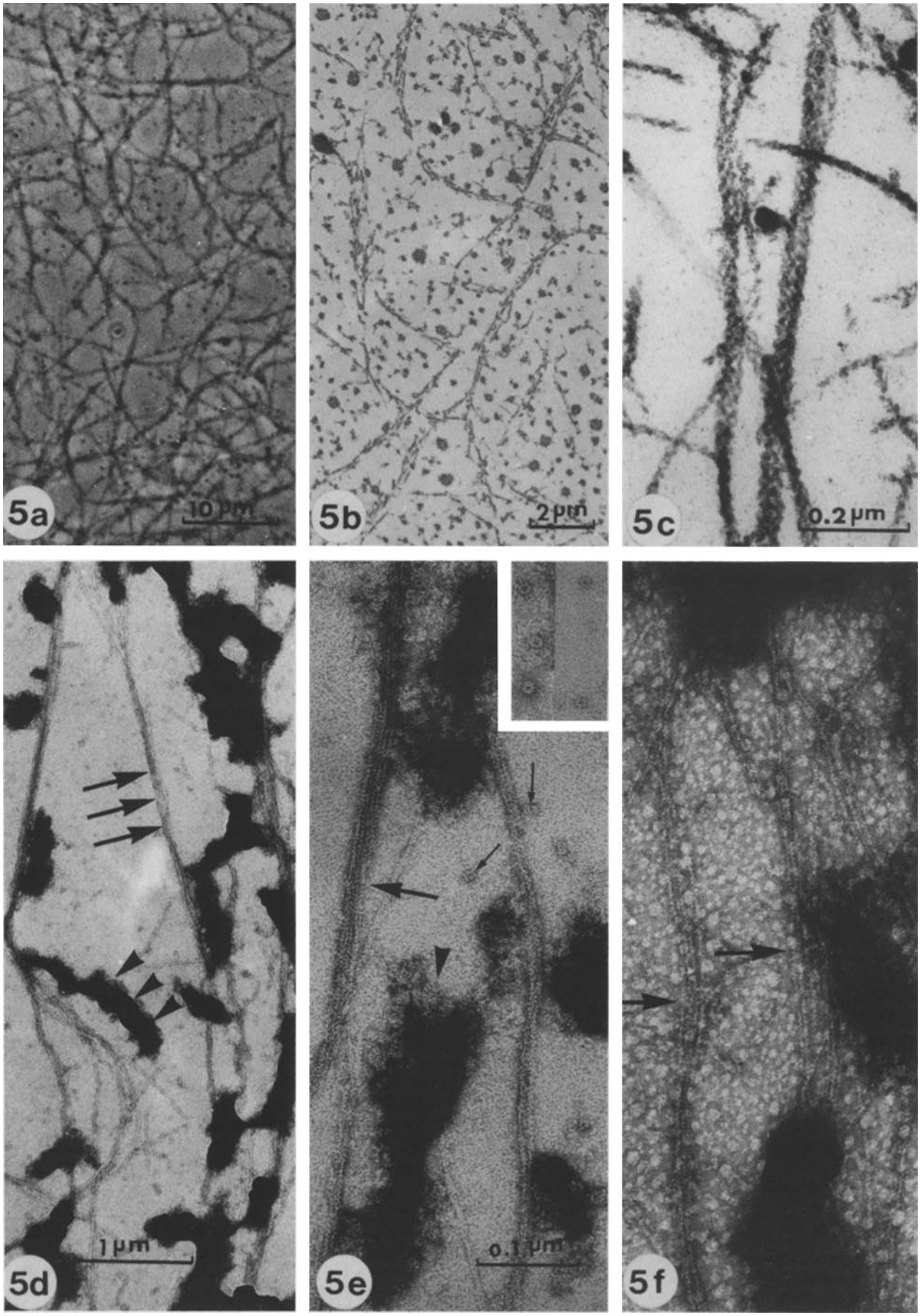
5a
10 µm
5b
2µm
5c
0.2µm
5d
1µm
5e
0.1 µm
5f

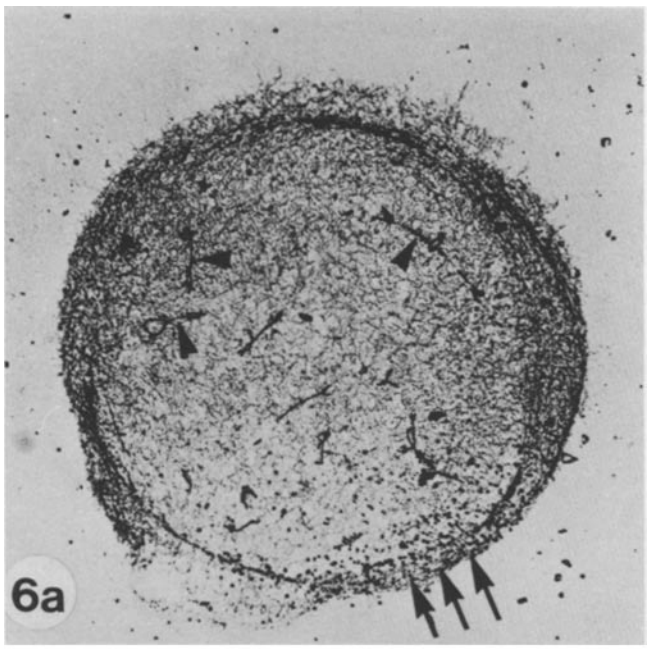

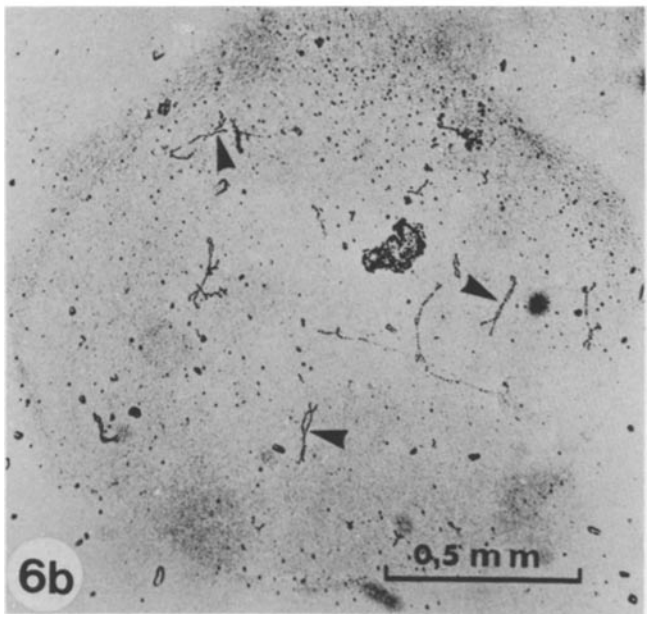

FIGURE 6 Immunocytochemical study of phalloidin-induced networks. Nuclei were incubated for 10 min in phalloidin (10^{-4} M), the nuclear envelope was removed, and the formed networks were processed for indirect immunoperoxidase as described in Materials and Methods. *a*, Actin antibody treatment (× 50); *b*, myosin antibody treatment (× 50). Arrowheads, lampbrush chromosomes; arrows, nucleoli. Note the difference of staining obtained with actin and myosin antibodies: the network, the chromosomes, and the nucleoli are strongly stained with antiactin. The network appears unstained with antimyosin at this magnification whereas chromosomes are faintly stained.

presence of EDTA (10 mM), which chelates mainly Mg^{++}, the nuclear sap remains relatively unchanged when observed at the level of the light microscope. On the other hand, EGTA (10 mM), which chelates more specifically Ca^{++}, leads to a gelation of the nuclear sap, as indicated by the fact that lampbrush chromosomes and other visible structures do not spread freely on the bottom of the chamber as they usually do after opening the germinal vesicle. Refringent fibrils are, however, not visible in phase-contrast microscopy. The structure of the nuclear sap treated by EGTA and observed by electron microscopy after Araldite embedding and thin sectioning is shown in Fig. 9*a*. Numerous thin filaments 6–10 nm in diameter are visible everywhere on the grids. Particles 80–100 nm in

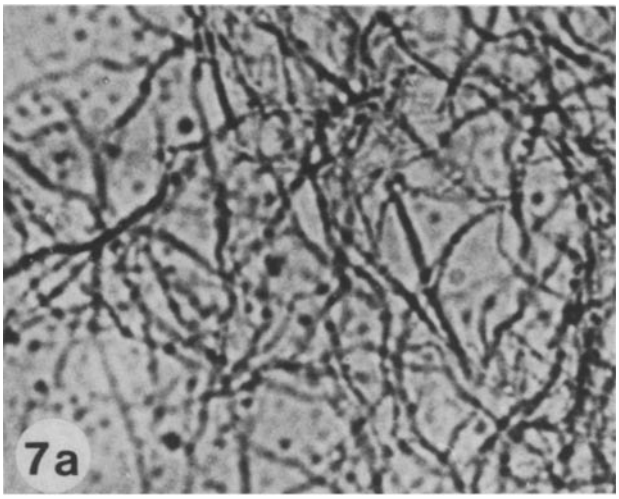

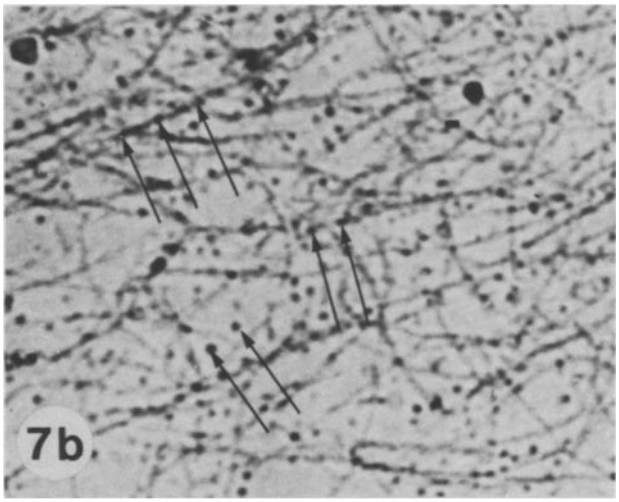

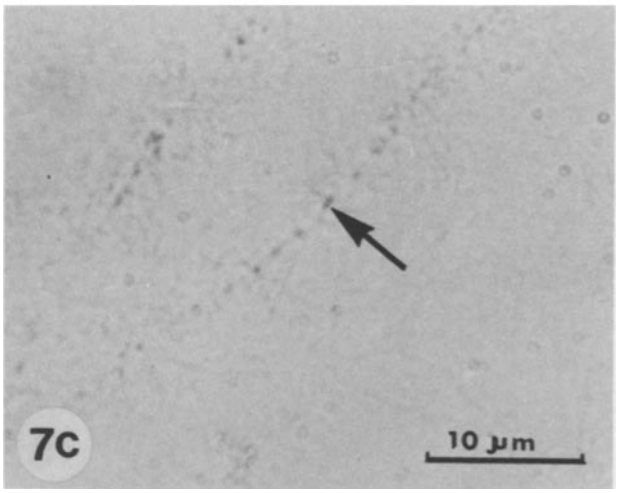

FIGURE 7 Immunocytochemical study of phalloidin-induced networks at a high magnification. × 2,000. Indirect immunoperoxidase treatment by (*a*) actin antibodies, (*b*) myosin antibodies, and (*c*) rat IgG antibodies used as a control. Cables are uniformly stained with antiactin (*a*), whereas antimyosin stains granules free or bound to the cables (*b*, arrows). No staining can be found in control preparations (*c*). Arrow in *c* shows part of an unstained lampbrush chromosome.

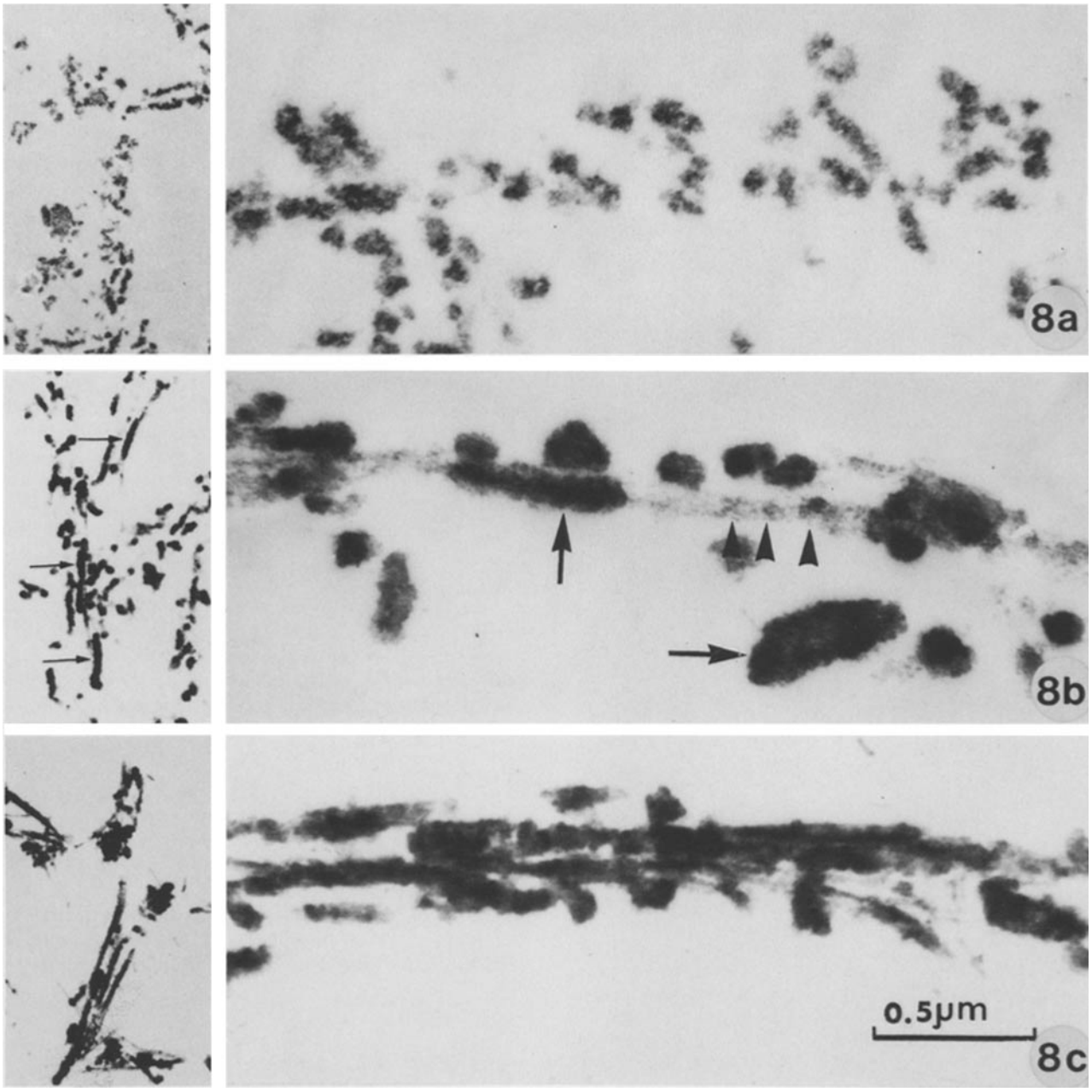

FIGURE 8 Immunocytochemical study of phalloidin-induced networks, electron microscopic observations. After indirect immunoperoxidase treatment, the networks were fixed with OsO_4 (1%), processed for electron microscopy as described in Materials and Methods, and observed at an acceleration voltage of 40 keV (× 54,000); *inset*, × 10,000). *a*, Control experiment, the network was treated by rat IgG antibodies. *b*, Myosin antibody treatment. *c*, Actin antibody treatment. The reaction product of the peroxidase activity corresponds to the electron-dense, black precipitates of diaminobenzidine. The intrinsic contrast of proteins fixed with OsO_4 is shown in *a*. Only the cable-bound particles are visible. These particles are stained with myosin antibodies (*b*, arrows). The cables are faintly stained in places with antimyosin antibodies, suggesting that some myosin molecules are present on the cables (*b*, arrowhead). Antiactin antibodies strongly stain the cables and the particles (*c*).

diameter are bound to these filaments. Large, spherical, electron-dense structures, which are probably nucleoli, also interact with the filaments as in nuclear sap prepared in TBS alone. The microfilaments formed in EGTA are indeed actin microfilaments, as demonstrated by S_1 decoration (Fig. 9*b*).

The type of cables observed in nuclei treated by phalloidin cannot be found in EGTA-treated nuclei. A more detailed study of EGTA-treated nuclei will be reported elsewhere. Mainly, results obtained by incubation of nuclei in Ca^{++}/EGTA buffers of various ratios indicate that the formation of microfilaments occurs below micromolar free concentrations of Ca^{++}. EGTA-induced microfilaments do not occur in nuclei preincubated for 20–30 min in TBS containing 5.10^{-5} M Ca^{++}, suggesting that globular actin has diffused out of the nuclei in this medium.

Modulation of Phalloidin Effect by ATP and Divalent Cations

ATP REQUIREMENT FOR CABLE FORMATION: To test the necessity of energy in the process of cable formation induced by phalloidin, we have tested the action of the non-hydrolysable ATP analogue ATPγS. In the presence of ATPγS (1-2 mM), phalloidin (10^{-4} M) does not transform the nuclear

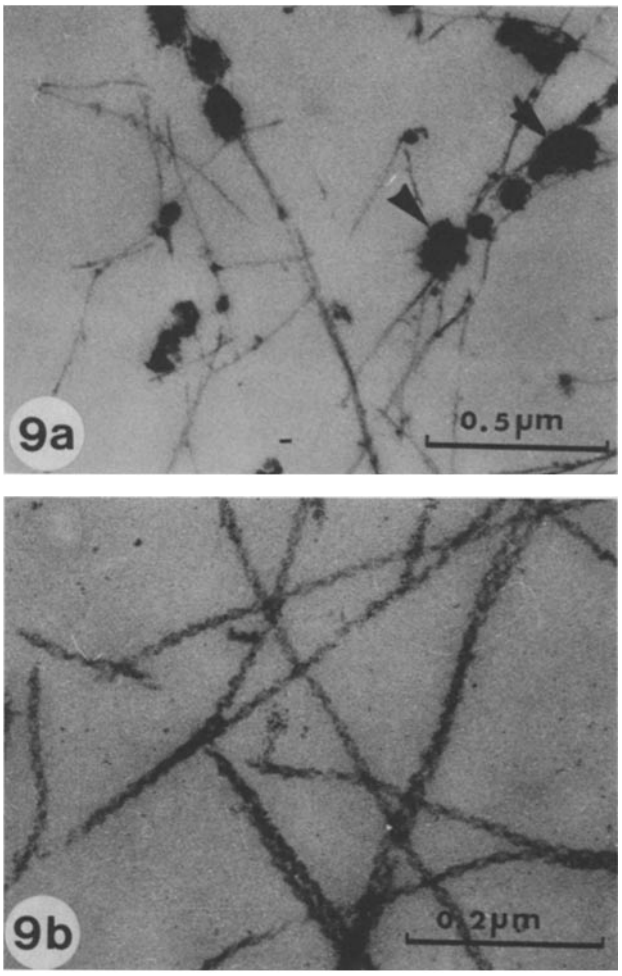

FIGURE 9 Structure of the nuclear sap treated with EGTA. Nuclei were incubated for 10 min in EGTA (10 mM), the nuclear envelope was reoved, and the gel was centrifuged in the chamber. The gel was then fixed with glutaraldehyde (2%) in TBS containing tannic acid (0.2%) for 10 min and processed for electron microscopy as described in Materials and Methods. (*a*) Individual microfilaments 6–10 nm in diameter are visible, to which particles are bound (arrowheads). × 40,000. (*b*) S_1 myosin subfragment decorates the microfilaments. × 100,000.

sap into a complex network of cables, nor is there gelation of the nuclear sap. When ATPγS (1 mM) is added to a forming network, the network will dissolve (the disappearance of cables can be followed by phase contrast microscopy). Fig. 5*f* shows an example of such a dissolving network adsorbed on a grid, stained with uranyl acetate, and observed in the electron microscope. Some 6-nm filaments are still associated, but more loosely than in the networks well visualized by phase contrast microscopy. Most microfilaments are free.

After 10–15 min in the presence of ATPγS, microfilaments are rarely found on electron microscope grids after staining with uranyl acetate. This dissolution process can be reversed (reappearance of cables in phase contrast microscopy) only by an equimolar concentration of ATP added shortly after ATPγS.

Finally, it is worth mentioning that highly coherent networks are not dissociated by ATPγS (when phalloidin action is prolonged for a period of time longer than 15 min).

DIVALENT CATION REQUIREMENTS OF PHALLOIDIN-INDUCED CABLE FORMATION: Phalloidin in the presence of EDTA does not induce the formation of cables visible in phase contrast microscopy. EGTA (10 mM), which chelates Ca^{++} ions more specifically, induces gelation of the nuclear sap by the formation of individual microfilaments (see above). Addition of phalloidin to nuclear sap in EGTA does not alter the structure of this gel; no association of individual microfilaments into cables is promoted.

Global Estimation of the Relative Amount of Nuclear G- and F-Actin by the DNAase I Inhibition Assay

G-actin has been shown to interact with DNAase I and inhibit its enzymatic activity in a few seconds. On the other hand, inhibition of DNAase I by F-actin is a much slower process, allowing the selective quantitation of G-actin (1).

To estimate the amount of G-actin in nuclei isolated in various buffers, a standard amount of DNAase I was added and the percent inhibition of the DNAase activity was measured. The total amount of actin per nucleus (G + F) was measured by incubating nuclei in actin-depolymerizing medium. The results obtained are reported in Fig. 10. The total amount of actin per nucleus estimated by this test corresponds to ~0.1 μg. More than 90% of actin is under a globular state in nuclei freshly isolated in K/Na solution or in TBS. 50% of actin is globular in nuclei isolated in TBS containing 10 mM EGTA. Globular actin has virtually disappeared from phalloidin (10^{-4} M)-treated nuclei.

DISCUSSION

The presence of G- and F-actin in large amounts in the nucleus of *Xenopus* oocytes was reported by Clark and Merriam (5) and Clark and Rosenbaum (6). They characterized this actin by biochemical, immunochemical, and morphological means. In the present work, we have confirmed and extended their finding in an other amphibian; the *Pleurodeles waltlii*. The actin has been characterized by morphological, immunocyto-

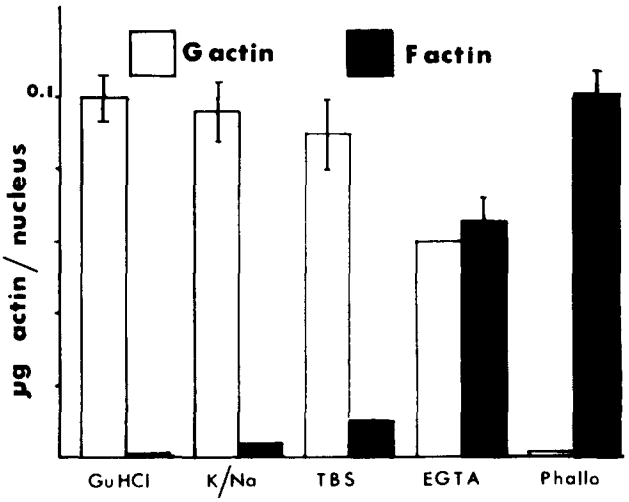

FIGURE 10 Quantitation of G- and F-actin in nuclei isolated under various conditions. Nuclei were isolated in various buffers, as described in Material and Methods, and assayed for DNAase I inhibitor activity. The amounts of G- and F-actins per nuclei isolated in the indicated buffers is reported. Histograms represent the average of three determinations. Vertical bars indicate standard error.

chemical, biochemical, and functional criteria. The presence of myosin has been suggested by immunocytochemical means.

We have found 0.1 μg of actin per nucleus using the DNAase I inhibition assay. This is close to the value reported by Clark and Rosenbaum (0.13 μg for *Xenopus* oocyte nuclei [6]). The nuclei used to quantitate actin by the DNAase I assay had an average radius of 200 μm, which gives an actin concentration close to 3 mg/ml in *Pleurodeles* nuclei. Again, this value is in fair agreement with the results obtained by Clark and Rosenbaum (4.5 mg/ml in *Xenopus* [6]).

Beyond actin and myosin characterization, our main aim was to investigate the possible regulatory mechanisms of the supramolecular forms taken by actin in the whole nuclear sap and the possible interactions of actin with nuclear structures or proteins. This information could, indeed, help us to understand the origin of the variations in consistency of the nuclear sap known to exist from one species to the other and in a given species, according to the physiological state of the individuals.

In vitro, purified actin is soluble (G-actin) at low ionic strength. It forms thin filaments 60–70 Å in diameter in 0.1 M KCl (F-actin). Divalent cations (1 mM Mg^{++} and 10^{-5} M Ca^{++}) have no obvious action on purified F-actin in 0.1 M KCl. Nuclear sap of oocyte nuclei was prepared in TBS containing 0.08 M KCl, 1 mM $MgCl_2$ and 5.10^{-5} M $CaCl_2$. Yet very few 60 Å filaments were observed by electron microscopy, and the DNAase I assay has shown that >90% of actin was under a globular state. This finding implies that, in the nuclear sap, actin is bound to proteins or structures that do not allow 60 Å filaments to form. Samples of nuclear sap observed by electron microscopy reveal the presence of a granular material. The size of the predominant particles ranged from 20–50 nm, which is close tothe size of the elementary subunits of ribonucleoprotein (RNP) in the nuclei of *Triturus* oocytes described by Malcolm and Sommerville (28) and Mott and Callan (31). Large particles (up to 300 nm) apparently formed of aggregated subparticles were also reported by the same authors.

The presence of actin has been reported in isolated RNP particles (2, 29). Therefore, the nonfilamentous nuclear actin may be present as two forms: (*a*) associated with RNP and other nuclear structures, and (*b*) in a soluble, diffusible form.

We have found two treatments which lead to a modification of the structure of the nuclear sap of nuclei isolated in TBS. (*a*) Phalloidin formed a dense network of actin cables in which nucleoli and chromosomes were trapped. (*b*) EGTA (Ca^{++} chelation mainly) formed a fine gel composed of individual microfilaments.

The presence of actin in the cables formed by addition of phalloidin to the nuclei is demonstrated by the morphology of these cables in the electron microscope, by decoration with S_1 subfragment, and by the heavy staining obtained with actin antibodies. The observation of whole networks stained with the actin antibody in microscopy at low magnification clearly shows the quantitative importance of actin in oocyte nuclei. Moreover, the chromosomes are strongly stained, as previously reported (21), as well as the nucleoli.

The large particles associated with these cables are composed of subunits, 20 nm in diameter, which strongly resemble the particles visible in untreated nuclear sap. We have not investigated in detail the nature of these particles, but they may well be RNP. The observation of negatively stained preparations previously treated by RNAase indicated that these particles were partially disrupted by the treatment. However, this result is still preliminary and needs to be confirmed by other approaches. Besides the 20-nm subparticles, numerous ring structures 10 nm in diameter, sometimes groups of two or three, are present between the cables. Their nature is unknown. From a morphological point of view they resemble the actin-binding protein of Hartwig and Stossel (15). In addition to containing actin, the particles bound to the cables seem to contain myosin, inasmuch as the faint staining of the network observed by light microscopy with myosin antibodies was found, in the electron microscope, to be mainly localized on these particles. This observation may indicate that myosin could play a role in cable-particle interactions. It is interesting to note that virtually all the G-actin measured by the DNAase I inhibition assay polymerizes into F-actin in the presence of phalloidin.

Concerning the functional behavior of the nuclear sap in response to phalloidin treatment, one point should be stressed; the addition of phalloidin to purified G-actin solutions results in the formation of individual F-actin filaments resistant to dissociation by 0.6 M KI (27, 43). It does not induce the formation of actin cables (27). Yet in the oocyte nucleus, actin cables were formed. This difference in behavior is of great significance because EGTA induces only the formation of individual actin microfilaments in the nuclear sap. Moreover, particles of the same kind as those found on phalloidin-induced cables were observed associated with the microfilaments formed by EGTA. This suggests that the formation of cables by phalloidin in the oocyte nuclei requires the presence of a set of proteins which associate individual microfilaments in the presence of Ca^{++}. The apparent presence of myosin on the cables and especially on the particles bound to the cables suggests that myosin could be involved in the association of microfilaments into cables.

This possibility is also supported by the fact that ATPγS, which impairs F-actin-myosin interaction (12), dissociates forming networks of cables and that Ca^{++} and Mg^{++} seem to be required to allow cable formation in the presence of phalloidin. To our knowledge, the role of myosin in cable formation has not yet been clearly defined except in one recent paper (41) where it is shown that heavy meromyosin (HMM) cross-links purified F-actin. Moreover, this reaction is facilitated by addition of ATP in micromolar concentration, and a ratio HMM to actin as low as 1/100 (wt/wt) is enough to form a strong gel composed of bundles of two, three, or even 10 microfilaments cross-linked by HMM.

In very low Ca^{++} concentration (excess EGTA), the G-actin of nuclei was found to form individual microfilaments usually cross-linked by aggregated electron-dense particles. The DNAase I inhibition assay indicates that, under such conditions, ~50% of the total nuclear actin is in a filamentous form. This strongly suggests that the presence of Ca^{++} in medium inhibits nuclear actin polymerization. This may be caused by the presence of a Ca^{++} binding protein which would inhibit cross-linking of actin filaments, leading to their destabilization in the nuclear environment (30, 44). Why all the nuclear actin does not polymerize into G-actin in low Ca^{++} could be explained in two ways, as already suggested by Clark and Merriam (5) and Clark and Rosenbaum (6) for nuclear actin in *Xenopus laevis*: (*a*) this actin is different in nature from muscle actin and will not polymerize spontaneously at this concentration; (*b*) actin is bound to proteins which inhibit its polymerization.

We will discuss elsewhere that, in fact, the interaction be-

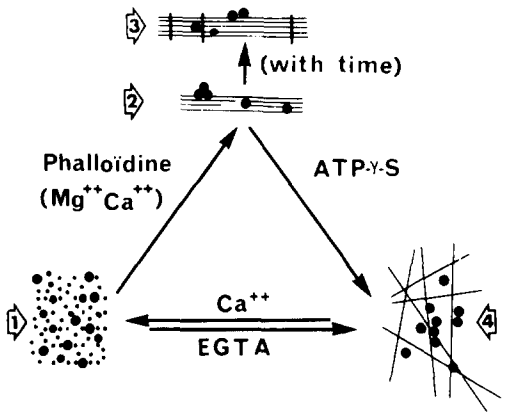

FIGURE 11 The various structural states of actin in the nucleus of *Pleurodeles* oocytes. (*1*) The granular state of nuclear saps isolated in TBS. Absence of filamentous structures. (*2*) Actin cables induced by phalloidin in the presence of Ca^{++} and Mg^{++}. (*3*) Actin cables stabilized by a putative actin-binding protein. (*4*) The individual microfilaments and their associated particles, formed in the presence of EGTA. Dark dots in *1–4* represent RNP-like particles.

tween actin and RNP may be of importance to explain the behavior of nuclear actin.

The scheme in Fig. 11 shows the various structural forms taken by actin and its putative associated proteins in nuclear sap isolated in various conditions. The results reported here indicate that a delicate equilibrium, probably maintained by Ca^{++}, ATP, and actin binding proteins, exists between G-actin, F-actin, and cables in oocyte nuclei. During the preparation of this paper, Clark and Rosenbaum (6) reported the presence of a gel composed of individual microfilaments in the nuclear sap of *Xenopus* oocytes. In *Pleurodeles*, we have found similar gels only in EGTA-treated nuclei. However, in the nuclei treated with phalloidin, nucleoli were usually found grouped in one region of the network. This polarity, which was revealed by the phalloidin treatment, was probably maintained in the native (untreated) nucleus by a small number of individual microfilaments interacting with the nucleoli, as observed by electron microscopy, in nuclei freshly isolated in TBS. The present results suggest that the structural state of nuclear actin is regulated in a manner similar to that which is known to occur in cytoplasmic extracts (for review see references 16 and 18). This does not mean that nuclear actin has no specific nuclear functions in oocyte nuclei. It seems that structural and functional interactions exist between the genomic material and contractile proteins. Further work is needed to elucidate the meaning of such interactions.

Finally, we would like to mention that the degree of structure of the nuclear sap varies throughout the oocyte life. This last fact is well illustrated by the surprising observation we made that, over 3 yr, between April and August, the nuclear sap of *Pleurodeles* oocytes often contained networks of actin cables without phalloidin addition. Interestingly, *Pleurodeles* females do not lay eggs spontaneously during this period of the year. This may suggest a possible relationship between the sexual cycle (hormonal cycle) and the physiological state of oocytes.

We would like to acknowledge the skillfull assistance of Mrs. Francoise Richard. We thank Dr. R. Whalen for the purified myosin S_1 subfragment.

This work has been supported by grant MRM/P283 from the Délégation à la Recherche Scientifique et Technique.

Received for publication 8 July 1980, and in revised form 3 October 1980.

REFERENCES

1. Blikstad, I., F. Markey, L. Carlsson, T. Persson, and U. Lindberg. 1978. Selective assay of monomeric and filamentous actin in cell extracts, using inhibition of deoxyribonuclease I. *Cell.* 15:935–943.
2. Brunel, C., and M. L. Lelay. 1979. Two dimensional analysis of proteins associated with heterogenous nuclear RNA in various animal cell lines. *Eur. J. Biochem.* 99:273–283.
3. Callan, H. G. 1963. The nature of lampbrush chromosomes. *Int. Rev. Cytol.* 15:1–34.
4. Callan, H. G. 1966. Chromosomes and nucleoli of the axolotl, *Ambystoma mexicanum*. *J. Cell Sci.* 1:85–107.
5. Clark, T. G., and R. W. Merriam. 1977. Diffusible and bound actin in nuclei of *Xenopus laevis* oocytes. *Cell.* 12:883–891.
6. Clark, T. G., and J. L. Rosenbaum. 1979. An actin filament matrix in hand-isolated nuclei of *Xenopus laevis* oocytes. *Cell.* 18:1101–1108.
7. Commings, D., and D. Harris. 1975. Nuclear proteins. I. Electrophoretic comparison of mouse nucleoli, heterochromatin, eurochromatin and contractile proteins. *Exp. Cell Res.* 96:161–179.
8. Cuatrecasas, P., M. Wilchek, and C. B. Anfinsen. 1968. Selective enzyme purification by affinity chromatography. *Proc. Natl. Acad. Sci. U. S. A.* 61:636–643.
9. Douvas, A. S., C. A. Harrington, and J. Bonner. 1975. Major nonhistone proteins of rat liver chromatin: preliminary identification of myosin, actin, tubulin and tropomyosin. *Proc. Natl. Acad. Sci. U. S. A.* 72:3902–3906.
10. Gabbiani, G., G. B. Ryan, J. P. Lamelin, P. Vassali, G. Majno, C. A. Bouvier, A. Cruchaud, and E. F. Luscher. 1973. Human smooth muscle auto-antibody: its identification as antiactin antibody and a study of its binding to nonmuscular cells. *Am. J. Pathol.* 72:473–488.
11. Goldstein, L., R. Rubin, and C. Ko. 1977. The presence of actin in nuclei: a critical appraisal. *Cell.* 12:601–608.
12. Goody, R. S., K. C. Holmes, H. G. Mannherz, B. Leigh, and G. Rosenbaum. 1975. Cross-bridge conformation as revealed by X-ray diffraction studies of insect flight muscles with ATP analogues. *Biophys. J.* 15:687–705.
13. Gordon, W. E. III, A. Burshnell, and K. Burridge. 1978. Characterization of the intermediate filaments of cultured cells using an autoimmune rabbit serum. *Cell.* 13:249–261.
14. Graham, R. C., and M. J. Karnovsky. 1966. The early stages of absorption of injected horseradish peroxydase into the proximal tubules of mouse kidney. Ultrastructural cytochemistry by a new technique. *J. Histochem. Cytochem.* 14:291–301.
15. Hartwig, J. H., and T. P. Stossel. 1975. Isolation and properties of actin, myosin and a new actin binding protein in rabbit alveolar macrophages. *J. Biol. Chem.* 250:5696–5705.
16. Hellewell, S. B., and D. L. Taylor. 1979. The contractile basis of ameboid movement. VI. The solation-contraction coupling hypothesis. *J. Cell Biol.* 83:633–648.
17. Herman, I. M., and T. D. Pollard. 1978. Actin localization in fixed dividing cells stained with fluorescent heavy meromyosin. *Exp. Cell Res.* 114:15–25.
18. Hitchkock, S. E. 1977. Regulation of motility in nonmuscle cells. *J. Cell Biol.* 74:1–15.
19. Jockusch, B. M., K. H. Kelley, R. K. Meyer, and M. M. Burger. 1978. An efficient method to produce specific anti-actin. *Histochemistry.* 55:177–184.
20. Karsenti, E., and P. Gounon. 1979. Lampbrush chromosomes: are they ATP-dependent contractile structures? *Biol. Cell.* 34:91–98.
21. Karsenti, E., P. Gounon, and M. Bornens. 1978. Immunocytochemical study of lampbrush chromosomes: presence of tubulin and actin. *Biol. Cell.* 31:219–224.
22. Karsenti, E., B. Guilbert, M. Bornens, and S. Avrameas. 1977. Antibodies to tubulin in normal nonimmunized animals. *Proc. Natl. Acad. Sci. U. S. A.* 74:3997–4001.
23. Karsenti, E., B. Guilbert, M. Bornens, S. Avrameas, R. Whalen, and D. Pantaloni. 1978. Detection of tubulin and actin in various cell lines by an immunoperoxidase technique. *J. Histochem. Cytochem.* 26:934–947.
24. Laemmli, U. K. 1970. Cleavage of structural proteins during the assembly of the head of bacteriophage T4. *Nature (Lond.).* 227:680–685.
25. Lestourgeon, W. M., R. Totten, and A. Forer. 1974. The nuclear acidic proteins in cell proliferation and differentiation. *In* Acidic Proteins of the Nucleus. J. L. Cameron, and J. R. Jeter, editors. Academic Press, Inc., New York. 159–190.
26. Lestourgeon, W. M., A. Forer, Y. Z. Yang, J. S. Bertram, and H. P. Rush. 1975. Major components of nuclear and chromosome nonhistone proteins. *Biochim. Biophys. Acta.* 379: 529–552.
27. Lengsfeld, A. M., I. Low, T. Wieland, P. Dancker, and W. Hasselbach. 1974. Interaction of phalloidin with actin. *Proc. Natl. Acad. Sci. U. S. A.* 71:2803–2807.
28. Malcolm, D. M., and J. Sommerville. 1974. The structure of chromosome-derived ribonucleoprotein in oocytes of *Triturus cristatus carnifex* (Laurenti). *Chromosoma (Berl.).* 48: 137–158.
29. Maundrell, K., and K. Scherrer.1979. Characterization of pre-messenger-RNA-containing nuclear ribonucleoprotein particles from avian erythroblasts. *Eur. J. Biochem.* 99:225–238.
30. Mimura, N., and A. Asano. 1979. Ca^{2+}-sensitive gelation of actin filaments by a new protein factor. *Nature (Lond.).* 282:42–48.
31. Mott, R. M., and H. G. Callan. 1975. An electron-microscope study of the lampbrush chromosomes of the newt *Triturus cristatus*. *J. Cell Sci.* 17:241–261.
32. Mommaerts, W. F. H. M., and R. G. Parrish. 1951. Studies on myosin. I. Preparation and criteria of purity. *J. Biol. Chem.* 188:545–552.
33. Norberg, R., K. Lidman, and A. Fagraeus. 1975. Effects of cytochalasin B on fibroblasts lymphoid cells and platelets revealed by human anti-actin antibodies. *Cell.* 6:507–512.
34. Paulin, D., J. F. Nicolas, M. Jacquet, H. Jakob, F. Gros, and F. Jacob. 1976. Comparative protein patterns in chromatins from mouse teratocarcinoma cells. *Exp. Cell Res.* 102:169–178.
35. Pollard, T. D., S. M. Thomas, and R. Niederman. 1974. Human platelet myosin. I. Purification by a rapid method applicable to other nonmuscle cells. *Anal. Biochem.* 60: 258–266.
36. Rubin, R. W., L. Goldstein, and C. Ko. 1978. Differences between nucleus and cytoplasm in the degree of actin polymerisation. *J. Cell Biol.* 77:698–700.
37. Rungger, D., E. Rungger-Brandle, C. Chaponnier, and G. Gabbiani. 1979. Intranuclear injection of anti-actin antibodies into Xenopus oocytes blocks chromosome condensation. *Nature (Lond.).* 282:320–321.

38. Spudich, J. A., and S. Watt. 1971. The regulation of rabbit skeletal muscle contraction. *J. Biol. Chem.* 246:4866–4871.
39. Szent-Gyorgy, A. 1951. Myosin. *In* Chemistry of Muscular Contraction. Academic Press, Inc., New York. 38–57.
40. Ternynck, T., and S. Avrameas. 1972. Polyacrylamide-protein immunoabsorbents prepared with glutaraldehyde. *FEBS (Fed. Eur. Biochem. Soc.) Lett.* 23:24–27.
41. Trinick, J., and G. Offer. 1979. Cross-linking of actin filaments by heavy meromyosin. *J. Mol. Biol.* 133:549–556.
42. Wehland, J., M. Osborn, and K. Weber. 1977. Phalloidin-induced actin polymerization in the cytoplasm of cultured cells interferes with cell locomotion and growth. *Proc. Natl. Acad. Sci. U. S. A.* 74:5613–5617.
43. Wieland, T., and H. Faulstich. 1978. Amatoxins, phallotoxins, phallolysin and antamanide: the biologically active components of poisonous amanita mushrooms. *Crit. Rev. Biochem.* 5:185–260.
44. Yin, H. L., and T. P. Stossel. 1979. Control of cytoplasmic actin gel-sol transformation by gelsolin, a calcium-dependent regulatory protein. Nature (*Lond.*). 281:583–586.